Ain Shams Engineering Journal (2016) 7, 441–452

Ain Shams University

Ain Shams Engineering Journal

www.elsevier.com/locate/asej
www.sciencedirect.com

ENGINEERING PHYSICS AND MATHEMATICS

Transient thermophoretic particle deposition on forced convective heat and mass transfer flow due to a rotating disk

M.S. Alam [a], S.M. Chapal Hossain [a], M.M. Rahman [b,*]

[a] Department of Mathematics, Jagannath University, Dhaka 1100, Bangladesh
[b] Department of Mathematics and Statistics, College of Science, Sultan Qaboos University, P.O. Box 36, P.C. 123 Al-Khod, Muscat, Oman

Received 6 June 2014; revised 17 March 2015; accepted 15 April 2015
Available online 6 June 2015

KEYWORDS

Forced convection;
Heat transfer;
Mass transfer;
Unsteady flow;
Rotating disk;
Thermophoresis

Abstract This paper investigates thermophoretic deposition of micron sized particles on unsteady forced convective heat and mass transfer flow due to a rotating disk. Using similarity transformations the governing nonlinear partial differential equations are transformed into a system of ordinary differential equations that are then solved numerically by applying Nachtsheim–Swigert shooting iteration technique along with sixth-order Runge–Kutta integration scheme. The effects of the pertinent parameters on the radial, tangential and axial velocities, temperature and concentration distributions, and axial thermophoretic velocity together with the local skin-friction coefficient, and local Nusselt number are displayed graphically. The inward axial thermophoretic deposition velocity (local Stanton number) is also tabulated. The obtained results show that axial thermophoretic velocity is increased with the increasing values of the thermophoretic coefficient, thermophoresis parameter, rotational parameter as well as unsteadiness parameter. The results also show that inward axial thermophoretic particle deposition velocity decreases with the increase of the Lewis number.

1. Introduction

Flow due to a rotating disk is encountered in many industrial, geothermal, geophysical, technological and engineering applications. A few of them are rotating heat exchangers, rotating disk reactors for bio-fuels production, computer disk drives and gas or marine turbines. The pioneering study of fluid flow due to an infinite rotating disk was carried out by von Karman [1]. He formulated the problem and introduced a famous transformation which reduced the governing partial

* Corresponding author. Tel.: +968 2414 1423; fax: +968 24141 1490.
E-mail addresses: dralamjnu@gmail.com (M.S. Alam), chapal707@gmail.com (S.M. Chapal Hossain), mansurdu@yahoo.com (M.M. Rahman).

Peer review under responsibility of Ain Shams University.

Production and hosting by Elsevier

http://dx.doi.org/10.1016/j.asej.2015.04.005

List of symbols

Cf	skin-friction coefficient
c_p	specific heat at constant pressure
C	concentration within the boundary layer
C_w	concentration at the surface of the disk
C_∞	concentration of the ambient fluid
D_B	Brownian diffusivity
F	dimensionless radial velocity
G	dimensionless tangential velocity
H	dimensionless axial velocity
k	thermal conductivity of the fluid
Kn	Knudsen number
N_t	thermophoresis parameter
Nu	Nusselt number
Pr	variable Prandtl number
q	velocity vector
q_w	surface heat flux
R	rotational parameter
Re	rotational Reynolds number
r	cylindrical radial coordinate
Sc	Schmidt number
St	Stanton number
t	time
T	temperature within the boundary layer
T_w	temperature at the surface of the disk
T_∞	temperature of the ambient fluid
u, v, w	velocities along radial, tangential and axial direction respectively
U_T	thermophoretic velocity along the radial direction
V_d^*	nondimensional thermophoretic particle deposition velocity
W_T	thermophoretic velocity along the axial direction
W_T^*	nondimensional thermophoretic velocity along the axial direction
z	axial coordinate
ρ	density of the fluid
μ	coefficient of dynamic viscosity
υ	kinematic viscosity
κ	thermophoretic coefficient
α	thermal diffusivity
η	similarity variable
δ	time dependent length scale
λ	unsteadiness parameter
λ_g	thermal conductivity of the fluid
λ_p	thermal conductivity of the diffused particles
φ	azimuthal coordinate
ϕ	dimensionless concentration
τ_r	radial shear stress
τ_t	tangential shear stress
θ	dimensionless temperature
Ω	angular velocity

differential equations into ordinary differential equations. Cochran [2] obtained asymptotic solutions for the steady hydrodynamic problem formulated by von Karman. Benton [3] improved Cochran's solutions and solved the unsteady problem. The problem of heat transfer from a rotating disk maintained at a constant temperature was first considered by Millsaps and Pohlhausen [4] for a variety of Prandtl numbers in the steady state. Sparrow and Gregg [5] studied the steady state heat transfer from a rotating disk maintained at a constant temperature to fluids at any Prandtl number. Attia [6] studied the problem of unsteady MHD flow near a rotating porous disk with uniform suction or injection. Maleque and Sattar [7] investigated the influence of variable properties on the physical quantities of the rotating disk problem by obtaining a self-similar solution of the Navier–Stokes equations along with the energy equation. Attia [8] investigated the steady flow over a rotating disk in porous medium with heat transfer. Rahman [9] studied convective hydromagnetic slip flow with variable properties due to a porous rotating disk. Zueco and Rubio [10] analyzed the network method to study magnetohydrodynamic flow and heat transfer about rotating disk. Recently, Rahman [11] studied thermophoretic deposition of nanoparticles due to a permeable rotating disk considering the effects of partial slip, magnetic field, thermal radiation, thermal-diffusion, and diffusion-thermo. It is observed that slip mechanism, thermal-diffusion, diffusion-thermo, magnetic field and radiation significantly control the thermophoretic particles deposition rate.

Thermophoresis, the motion of suspended particles in a fluid induced by a temperature gradient, is of practical importance in a variety of industrial and engineering applications such as design of thermal precipitators, study on the behavior of soot or seeding particles in combustion systems, nuclear reactor safety, gas cleaning, chemical or physical vapor deposition and microcontamination control, etc. Due to the practical importance of thermophoresis phenomenon many researchers (Goren [12], Talbot et al. [13], Mills et al. [14], Jia et al. [15], Chiou and Cleaver [16], Tsai [17], Postelnicu [18] and the references therein) have studied and reported results on this topic considering various flow conditions in different geometries. Alam et al. [19–21] studied thermophoretic particle deposition on two dimensional hydromagnetic heat and mass transfer flow over an inclined flat plate with various flow conditions. Rahman and Postelnicu [22] studied the effects of thermophoresis on steady forced convective laminar flow of a viscous incompressible fluid over a rotating disk. Rahman et al. [23] studied the thermophoresis particle deposition on unsteady two-dimensional forced convective heat and mass transfer flow along a wedge with variable viscosity and variable Prandtl number whereas Postelnicu [24] studied the thermophoresis particle deposition in natural convection over inclined surface in a porous media.

The objective of the present paper was to extend the work of Rahman and Postelnicu [22] for unsteady case and to investigate the deposition mechanism of micron-sized particles due to thermophoresis on transient forced convective heat and mass transfer flow over an impermeable rotating disk whose surface temperature is lower than the temperature of its surrounding fluid. Using similarity transformations the governing equations for flow, heat and mass transfer have been transformed into a system of ordinary differential equations that

are solved numerically by applying Nachtsheim–Swigert shooting iteration technique along with sixth-order Runge–Kutta integration scheme. To the best of the authors' knowledge no research has come out considering the above-stated model and flow conditions.

2. Flow analysis and mathematical formulation

In a non-rotating cylindrical polar frame of reference (r, φ, z), where z is the vertical axis in the cylindrical coordinates system with r and φ as the radial and tangential axes respectively, let us consider a disk that rotates with constant angular velocity Ω about the z axis. The disk is placed at $z = 0$, and a viscous incompressible Newtonian fluid occupies the region $z > 0$. The flow configurations and coordinate system are shown in Fig. 1. The components of the flow velocity $\mathbf{q}$ are (u, v, w) in the direction of increasing (r, φ, z) respectively. The surface of the rotating disk is maintained at a uniform temperature T_w and far away from the wall, and the free stream temperature is $T_\infty (> T_w)$. The species concentration at the surface is maintained uniform at C_w, which is taken to be zero (a clean surface) and that of the ambient fluid is assumed to be C_∞. At $t < 0$ the fluid is at rest, and at constant temperature and concentration the disk does not rotate. At $t = 0$ the disk is instantaneously put into motion (impulsively accelerated) at constant angular velocity, impulsively cooled at a lower uniform temperature and the discrete phase is impulsively removed at the disk surface. Only because of this the flow is actually transient during a very small time interval before reaching the well known steady-state conditions.

The effects of thermophoresis are being taken into account to help in the understanding of the mass deposition variation on the surface. We further assume that

(i) the mass flux of particles is sufficiently small so that the main stream velocity and temperature fields are not affected by the thermophysical processes experienced by the relatively small number of particles,

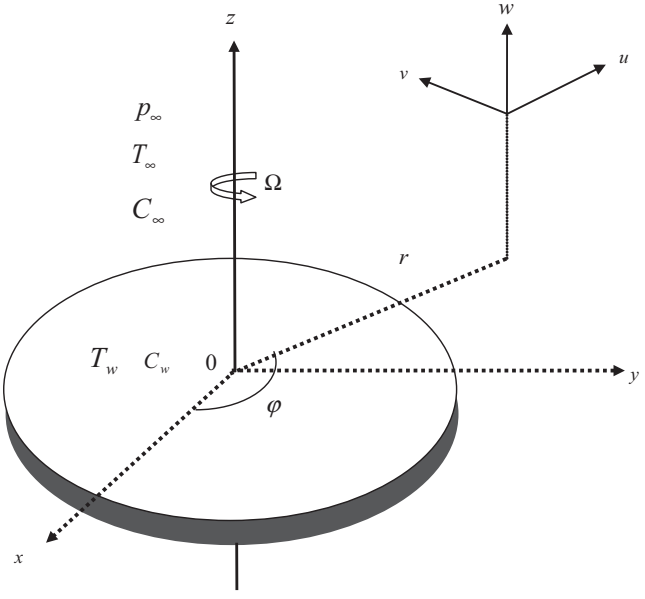

Figure 1 Flow configurations and coordinate system.

(ii) when particles hit the disk surface, they will be absorbed by it and none will be bounced back,

(iii) due to the boundary layer behavior the temperature gradient in the z-direction is much larger than that in the r-direction and hence only the thermophoretic velocity component which is normal to the surface is of importance,

(iv) the fluid has constant kinematic viscosity and thermal diffusivity,

(v) the particle diffusivity is assumed to be constant, and the concentration of particles is sufficiently diluted to assume that particle coagulation in the boundary layer is negligible, and

(vi) the flow is unsteady and axially symmetric.

Following the assumptions stated above, the mass, momentum, energy and particle concentration equations can be written as (see also Rahman and Postelnicu [22])

$$\frac{\partial u}{\partial r} + \frac{u}{r} + \frac{\partial w}{\partial z} = 0, \tag{1}$$

$$\frac{\partial u}{\partial t} + u\frac{\partial u}{\partial r} - \frac{v^2}{r} + w\frac{\partial u}{\partial z} = -\frac{1}{\rho}\frac{\partial p}{\partial r} + \upsilon\left(\frac{\partial^2 u}{\partial r^2} + \frac{1}{r}\frac{\partial u}{\partial r} - \frac{u}{r^2} + \frac{\partial^2 u}{\partial z^2}\right), \tag{2}$$

$$\frac{\partial v}{\partial t} + u\frac{\partial v}{\partial r} + \frac{uv}{r} + w\frac{\partial v}{\partial z} = \upsilon\left(\frac{\partial^2 v}{\partial r^2} + \frac{1}{r}\frac{\partial v}{\partial r} - \frac{v}{r^2} + \frac{\partial^2 v}{\partial z^2}\right), \tag{3}$$

$$\frac{\partial w}{\partial t} + u\frac{\partial w}{\partial r} + w\frac{\partial w}{\partial z} = -\frac{1}{\rho}\frac{\partial p}{\partial z} + \upsilon\left(\frac{\partial^2 w}{\partial r^2} + \frac{1}{r}\frac{\partial w}{\partial r} + \frac{\partial^2 w}{\partial z^2}\right), \tag{4}$$

$$\frac{\partial T}{\partial t} + u\frac{\partial T}{\partial r} + w\frac{\partial T}{\partial z} = \alpha\left(\frac{\partial^2 T}{\partial r^2} + \frac{1}{r}\frac{\partial T}{\partial r} + \frac{\partial^2 T}{\partial z^2}\right), \tag{5}$$

$$\frac{\partial C}{\partial t} + u\frac{\partial C}{\partial r} + w\frac{\partial C}{\partial z} = D_B\left(\frac{\partial^2 C}{\partial r^2} + \frac{1}{r}\frac{\partial C}{\partial r} + \frac{\partial^2 C}{\partial z^2}\right) - \frac{\partial}{\partial r}(U_T C) - \frac{\partial}{\partial z}(W_T C), \tag{6}$$

where u, v, and w are the velocity components in the r, φ and z directions respectively, υ is the kinematic viscosity, ρ is the density of the fluid, p is the pressure, T is the temperature of the fluid inside the thermal boundary layer while C is the corresponding concentrations, D_B is the Brownian diffusivity, and U_T and W_T are the thermophoretic velocities along the radial and axial directions respectively.

The thermophoretic velocities U_T and W_T that appear in Eq. (6), can be written as (see also, Rahman and Postelnicu [22])

$$U_T = -\frac{\kappa\upsilon}{T}\frac{\partial T}{\partial r}, \quad W_T = -\frac{\kappa\upsilon}{T}\frac{\partial T}{\partial z}, \tag{7}$$

where κ is the thermophoretic coefficient which ranges in value from 0.2 to 1.2 as indicated by Batchelor and Shen [25] and is defined from the theory of Talbot et al. [26] by

$$\kappa = \frac{2C_s(\lambda_g/\lambda_p + C_t Kn)[1 + Kn(C_1 + C_2 e^{-C_3/Kn})]}{(1 + 3C_m Kn)(1 + 2\lambda_g/\lambda_p + 2C_t Kn)} \tag{8}$$

where $C_1, C_2, C_3, C_m, C_s, C_t$ are constants, λ_g and λ_p are the thermal conductivities of the fluid and diffused particles, respectively and Kn is the Knudsen number.

2.1. Boundary conditions

(i) On the surface of the disk ($z = 0$):

$$u = 0, \quad v = \Omega r, \quad w = 0, \quad p = \text{constant} = 0, \quad T = T_w, \quad C = C_w = 0, \tag{9a}$$

(ii) Matching with the quiescent free stream ($z \to \infty$):

$$u = 0, \quad v = 0, \quad T = T_\infty, \quad C = C_\infty. \tag{9b}$$

We look for similarity solutions of Eqs. (1)–(6) together with the boundary conditions (9) to introduce the following similarity transformations:

$$\left.\begin{aligned} &\eta = \tfrac{z}{\delta}, \quad u = \Omega r F(\eta), \quad v = \Omega r G(\eta), \quad w = \tfrac{\upsilon}{\delta} H(\eta), \\ &p = -\rho\upsilon\Omega P(\eta), \quad \theta(\eta) = \tfrac{T_\infty - T}{T_\infty - T_w}, \quad \phi(\eta) = \tfrac{C}{C_\infty}. \end{aligned}\right\} \tag{10}$$

where δ is a scale factor and is a function of time as $\delta = \delta(t)$ (see Sattar and Hossain [27], and Rahman et al. [23]).

Substituting Eq. (10) into Eqs. (1)–(6), we obtain the following differential equations:

$$H' + 2RF = 0, \tag{11}$$

$$F'' - HF' - R\left(F^2 - G^2\right) + \lambda\eta F' = 0, \tag{12}$$

$$G'' - HG' - 2RFG + \lambda\eta G' = 0, \tag{13}$$

$$H'' - HH' + RP' + \lambda\eta H' = 0, \tag{14}$$

$$\theta'' - PrH\theta' + \lambda\eta\theta' = 0, \tag{15}$$

$$\phi'' - ScH\phi' - \kappa ScN_t(1 - N_t\theta)^{-1}(\theta''\phi - \theta'\phi') + \lambda\eta\phi' = 0, \tag{16}$$

with the transformed boundary conditions as

$$F = 0, \quad G = 1, \quad H = 0, \quad P = 0, \quad \theta = 1, \quad \phi = 0, \text{ at } \eta = 0, \tag{17a}$$

$$F = 0, \quad G = 0, \quad \theta = 0, \quad \phi = 1, \text{ as } \eta \to \infty. \tag{17b}$$

The dimensionless parameters introduced in the above equations are as follows: $\lambda = \frac{\delta}{\upsilon}\frac{d\delta}{dt}$ is the unsteadiness parameter, $R = \frac{\Omega\delta^2}{\upsilon}$ is the rotational parameter, $Pr = \frac{\upsilon}{\alpha}$ is the Prandtl number, $N_t = \frac{T_\infty - T_w}{T_\infty}$ is the thermophoresis parameter and $Sc = \frac{\upsilon}{D_B}$ is the Schmidt number and prime(s) denote differentiation with respect to η.

It is good to mention that to make Eqs. (12)–(16) similar we have to consider $\frac{\delta}{\upsilon}\frac{d\delta}{dt} = \lambda$ as constant. By integrating we obtain $\delta = \sqrt{2\upsilon\lambda t}$ where the constant of integration is determined through the condition that $\delta = 0$ when $t = 0$. It thus appears that the length scale $\delta = \sqrt{2\upsilon\lambda t}$ is consistent with the usual length scale considered for various non-steady flows (Schlichting [29]). Since δ is a scaling factor as well as a similarity parameter, any value of λ in $\delta = \sqrt{2\upsilon\lambda t}$ would not change the nature of the solutions except that the scale would be different.

3. Parameters of engineering interest

The parameters of engineering interest for the present problem are the skin-friction coefficient, the Nusselt number, the thermophoretic velocity, the thermophoretic particle deposition velocity and the Stanton number which are obtained from the following expressions.

The radial shear stress τ_r and tangential shear stress τ_t are defined by

$$\tau_r = \left[\mu\left(\frac{\partial u}{\partial z} + \frac{\partial w}{\partial r}\right)\right]_{z=0} = \frac{\mu\Omega r}{\delta}F'(0), \tag{18}$$

$$\tau_t = \left[\mu\left(\frac{\partial v}{\partial z} + \frac{1}{r}\frac{\partial w}{\partial \varphi}\right)\right]_{z=0} = \frac{\mu\Omega r}{\delta}G'(0). \tag{19}$$

Hence the skin-frictions ($Cf = \tau/\rho\Omega^2 r^2$) along the radial and tangential directions are obtained as

$$Cf_r Re = F'(0), \tag{20}$$

Table 1 Comparison of the values of $F(\eta), G(\eta)$ and $-H(\eta)$ with White [31] without heat and mass transfer for $\lambda = 0$, and $R = 1$.

η	$F(\eta)$		$G(\eta)$		$-H(\eta)$	
	Present	White [31]	Present	White [31]	Present	White [31]
0.0	0.00000000	0.0000	1.00000000	1.0000	0.00000000	0.0000
1.0	0.18002352	0.1801	0.47666771	0.4766	0.26534785	0.2655
3.0	0.05655563	0.0581	0.08423853	0.0845	0.74391508	0.7452
5.0	0.01022057	0.0108	0.01369313	0.0144	0.85594800	0.8594

Table 2 Comparison of the values of $F'(0), -G'(0)$ and $-\theta'(0)$ with Kelson and Desseaux [32] when $\lambda = 0, R = 1$ and $Pr = 0.71$ in the absence of mass transfer and suction parameter.

$F'(0)$		$-G'(0)$		$-\theta'(0)$	
Kelson and Desseaux [32]	Present	Kelson and Desseaux [32]	Present	Kelson and Desseaux [32]	Present
0.510233	0.51022378	0.615922	0.61592380	0.325856	0.32637889

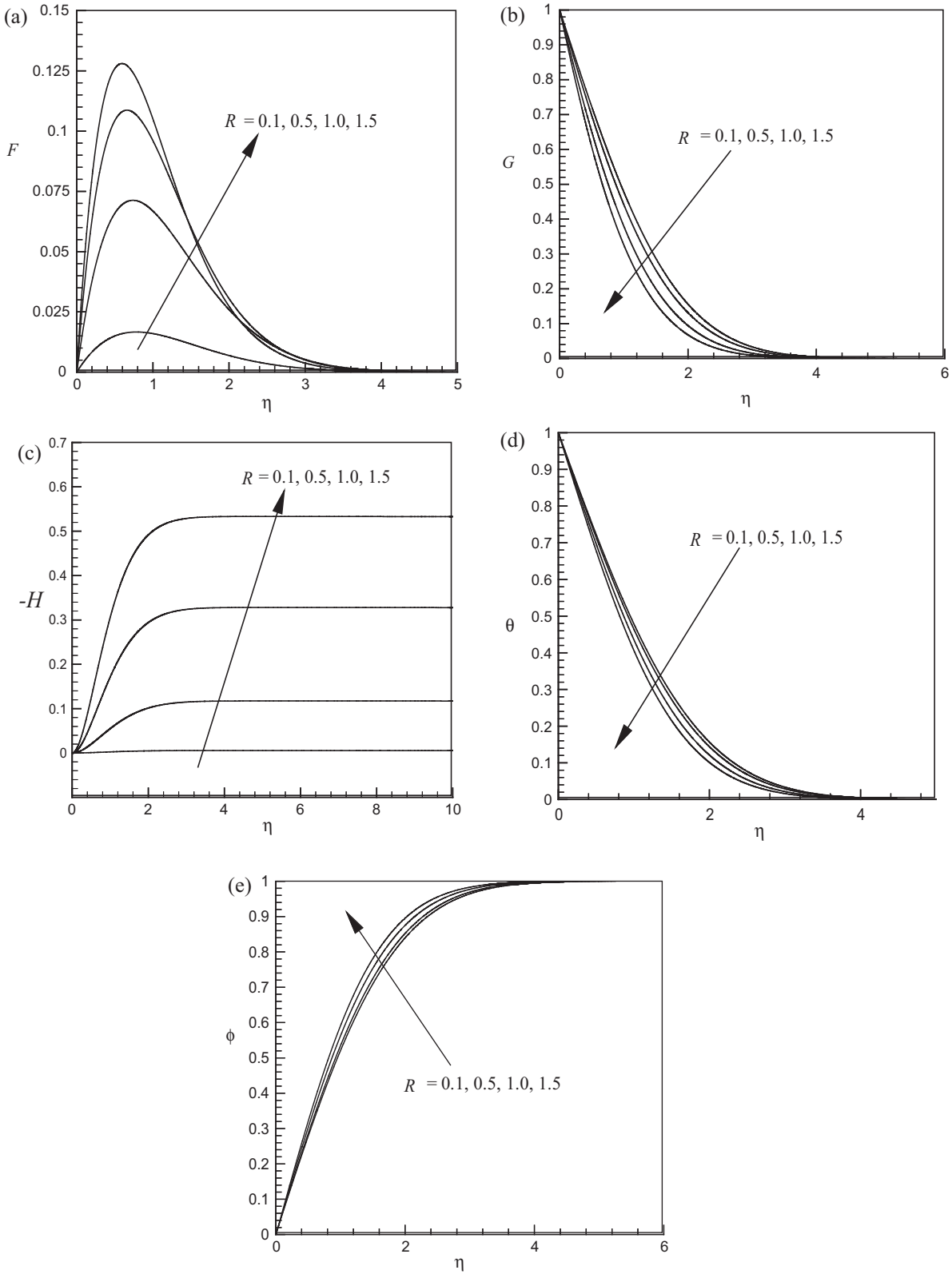

Figure 2 Variation of (a) radial velocity, (b) tangential velocity, (c) axial velocity, (d) temperature profile and (e) concentration profile for several values of R.

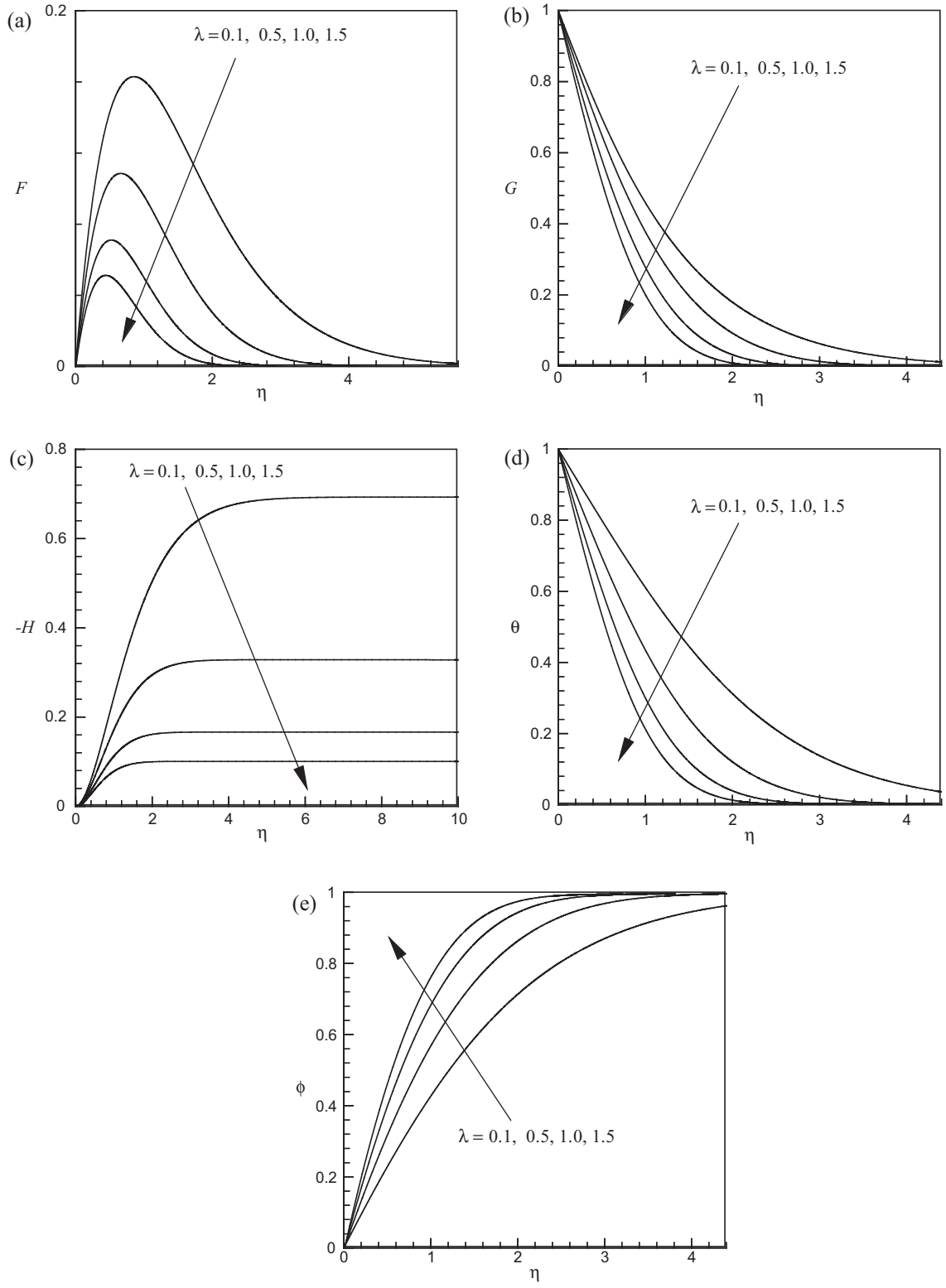

Figure 3 Variation of (a) radial velocity, (b) tangential velocity, (c) axial velocity, (d) temperature profile and (e) concentration profile for several values of λ.

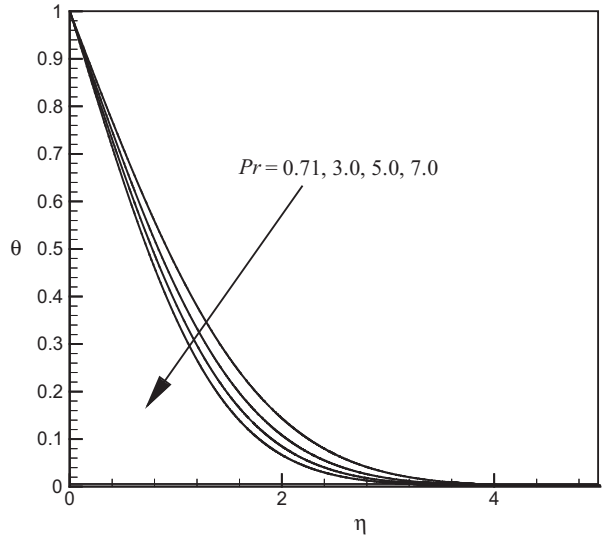

Figure 4 Temperature profile for several values of Pr.

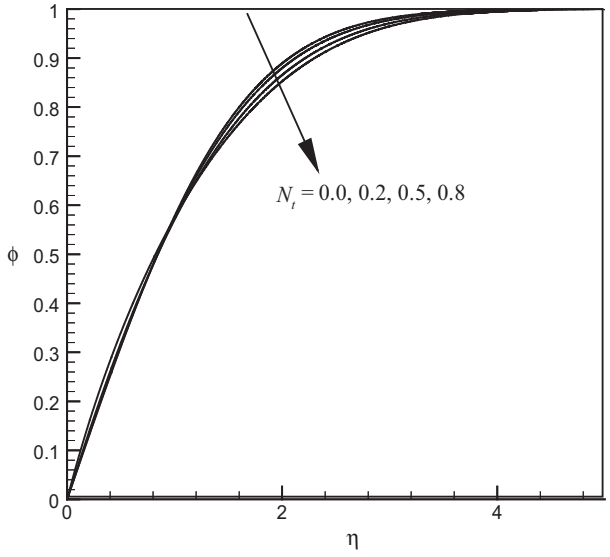

Figure 6 Concentration profiles for several values of N_t.

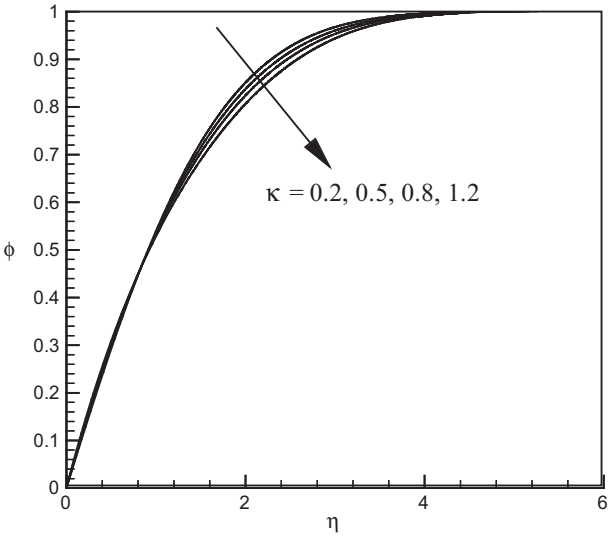

Figure 5 Concentration profiles for several values of κ.

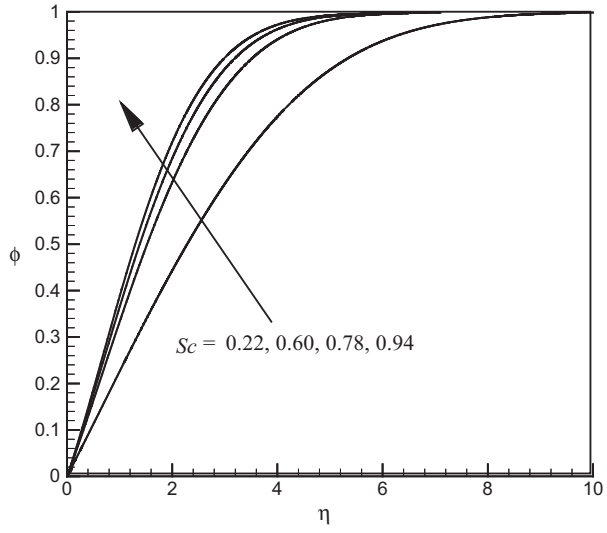

Figure 7 Concentration profiles for several values of $Sc < 1$.

$$Cf_t Re = G'(0), \tag{21}$$

where $Re = \Omega r\delta/\upsilon$ is the rotational Reynolds number.

The rate of heat transfer from the disk surface to the fluid is computed by the application of Fourier's law as given below

$$q_w = -k\left(\frac{\partial T}{\partial z}\right)_{z=0} = -k\frac{(T_\infty - T_w)}{\delta}\theta'(0). \tag{22}$$

Hence the Nusselt number is obtained as

$$Nu = \frac{\delta q_w}{k(T_\infty - T_w)} = -\theta'(0). \tag{23}$$

Thermophoretic velocities at the surface of the disk along the radial and axial directions are evaluated as

$$U_T]_{z=0} = 0, \quad W_T]_{z=0} = -\frac{\upsilon}{\delta}\frac{\kappa N_t}{(1-N_t)}\theta'(0). \tag{24}$$

Therefore a non-dimensional axial thermophoretic velocity can be written as

$$W_T^* = \frac{W_T\delta}{\upsilon} = -\frac{\kappa N_t}{(1-N_t)}\theta'(0). \tag{25}$$

Thermophoretic particle deposition velocity at the surface of the disk is evaluated by

$$V_d = \left(\frac{J_w}{C_\infty}\right)_{z=0} = -\frac{D_B}{\delta}\phi'(0), \text{ where}$$
$$J_w = -D_B\left(\frac{\partial C}{\partial z}\right)_{z=0} = -\frac{D_B C_\infty}{\delta}\phi'(0). \tag{26}$$

Therefore non-dimensional thermophoretic particle deposition velocity is evaluated as

$$V_d^* = \frac{V_d\delta}{\upsilon} = -(1/Sc)\phi'(0). \tag{27}$$

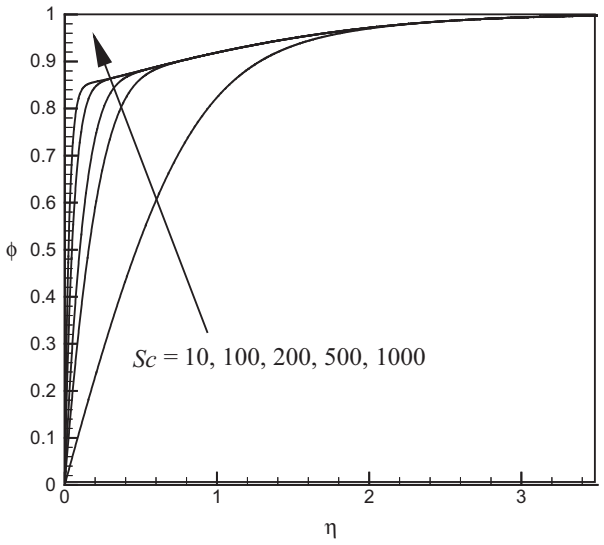

Figure 8 Concentration profiles for several values of $Sc >> 1$.

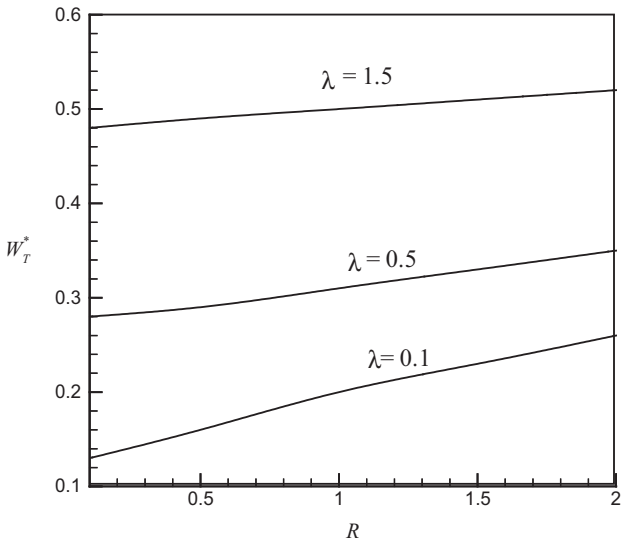

Figure 10 W_T^* versus R for different values of λ.

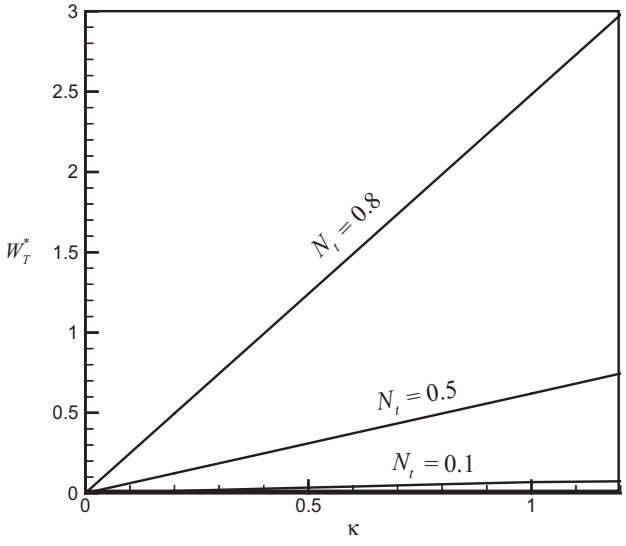

Figure 9 W_T^* versus κ for different values of N_t.

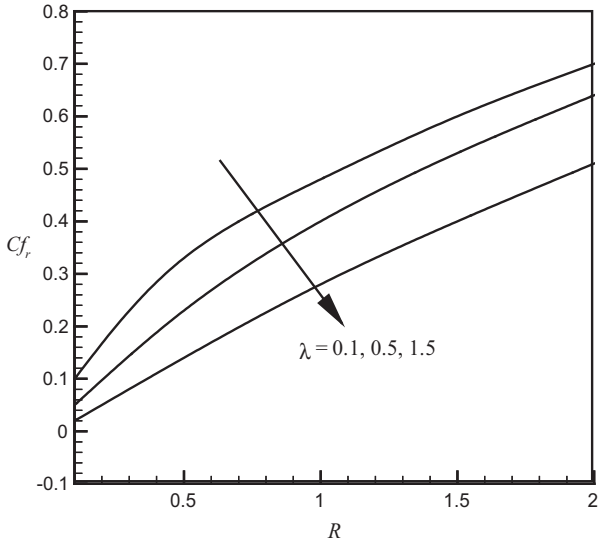

Figure 11 Cf_r versus R for different values of λ.

The negative sign in Eq. (27) represents that particle deposition will take place at the surface of the disk from the hotter region to the colder region i. e. from the fluid to the disk along the inward axial direction.

Now the local Stanton number is defined as

$$St = -\frac{J_w \delta}{C_\infty \upsilon} = (1/Sc)\phi'(0). \tag{28}$$

Comparing (27) and (28) we find that

$$St = -V_d^*. \tag{29}$$

4. Numerical simulations

The set of Eqs. (11)–(16) are nonlinear and coupled, so the system cannot be solved analytically. We dropped Eq. (14) from the system as it can be used for calculating pressure once F and H are known from the rest of the equations. Therefore Eqs. (11)–(13) and (15), (16) with boundary conditions (17) have been solved numerically by using sixth order Runge–Kutta method along with Nachtsheim–Swigert [30] shooting iteration technique (for detailed discussion of the method see Alam et al. [28]) with R, λ, Pr, κ, Nt and Sc as prescribed parameters. A step size of $\Delta\eta = 0.001$ was selected to be satisfactory for a convergence criterion of 10^{-6} in all cases. The value of η_∞ was found to each iteration loop by the statement $\eta_\infty = \eta_\infty + \Delta\eta$. The maximum value of η_∞ to each group of parameters R, λ, Pr, κ, Nt and Sc was determined when the value of the unknown boundary conditions at $\eta = 0$ does not change to a successful loop with an error less than 10^{-6}.

4.1. Code verification

When $\lambda = 0$ (i. e. for steady case), $R = 1$ and in the absence of heat and mass transfer, the present problem exactly coincides

with those (Eqs. 3–184 and 3–185) of White [31]. To assess the accuracy of the present code, we have calculated the values of F, G and $-H$ for different values of η in the absence of heat and mass transfer. Table 1 presents a comparison of the data obtained in the present work and those obtained by White [31]. It is clearly observed that very good agreement between the results exists.

It can further be noted that in the absence of mass transfer and for a steady case $\lambda = 0$, and $R = 1, Pr = 0.71$ the present problem coincides with that of Kelson and Desseaux [32]. In Table 2 we have also calculated the values of $F'(0), -G'(0)$ and $-\theta'(0)$ when $w_s = 0$ in the model of Kelson and Desseaux [32]. It is clearly observed that very good agreement between the results exists. This lends confidence in the present numerical method.

5. Results and discussion

In order to investigate the effects of the pertinent parameters such as rotational parameter R, unsteadiness parameter λ, Prandtl number Pr, thermophoretic coefficient κ, thermophoresis parameter N_t and Schmidt number Sc on the flow and heat, mass transfer characteristics are presented graphically as well as in tabulated form. The default values of the other parameters throughout the simulation are considered as $R = 1.0, \lambda = 0.5, N_t = 0.5, \kappa = 0.5, Pr = 0.71$, and $Sc = 10$ unless otherwise specified.

The effects of rotational parameter R on the dimensionless radial, tangential, inward axial velocity, temperature and concentration profiles are shown in Fig. 2(a)–(e) respectively. From these figures we observe that the radial, inward axial velocity and concentration profiles increase whereas both the tangential velocity and temperature profiles decrease with increasing values of the rotational parameter.

In Fig. 3(a)–(e) the influence of unsteadiness parameter λ on the dimensionless radial, tangential, inward axial velocity, temperature and concentration profiles across the boundary layer is displayed respectively. From these figures we observe that the radial, tangential, inward axial velocity and temperature profiles decrease whereas concentration profiles increase with increasing values of the unsteadiness parameter.

The influence of Prandtl number Pr on the temperature profiles within the boundary layer is depicted in Fig. 4. The Prandtl number defines the relative effectiveness of the momentum transport by diffusion in the hydrodynamic (velocity) boundary layer to the energy transported by thermal diffusion in the thermal boundary layer. According to the definition of Prandtl number high Pr fluids possess lower thermal conductivities which reduces the conduction heat transfer and increases temperature variations at the wall. Low Pr fluids have higher thermal conductivities and hence for $Pr < 1$, the thermal boundary layer will be thicker than the velocity boundary layer. Conversely for $Pr > 1$, the thermal boundary layer will be thinner than the velocity boundary layer. For the special case of $Pr = 1$, the two boundary layers will approximately of equal extent. An increase in Pr from 0.71, through 3, 5, 7, as shown in Fig. 4, therefore causes a strong decrease in temperature function θ, throughout the flow domain. With larger Pr values, thermal diffusivity is much less than the momentum diffusivity causing a decrease in temperature in the boundary layer.

The effect of the thermophoretic coefficient κ on the concentration profile is shown in Fig. 5. Fig. 3 reveals that for the studied parametric conditions an increase in the thermophoretic coefficient κ is to decrease the slope of the concentration profiles except very close to the surface of the disk ($\eta < 0.9$), whereas these profiles increase with the increase values of κ. This is due to the fact that thermophoresis has a suction-like effect on particles for a cold surface. This result is consistent with the work of Rahman and Postelnicu [22], for a steady flow.

In order to examine the effect of thermophoresis on particle deposition onto a rotating disk surface, the concentration profiles are displayed in Fig. 6, for thermophoresis parameter N_t. From this figure it is clear that the concentration profiles are decreased when temperature ratios are increased. This is because when large temperature difference exists, then the

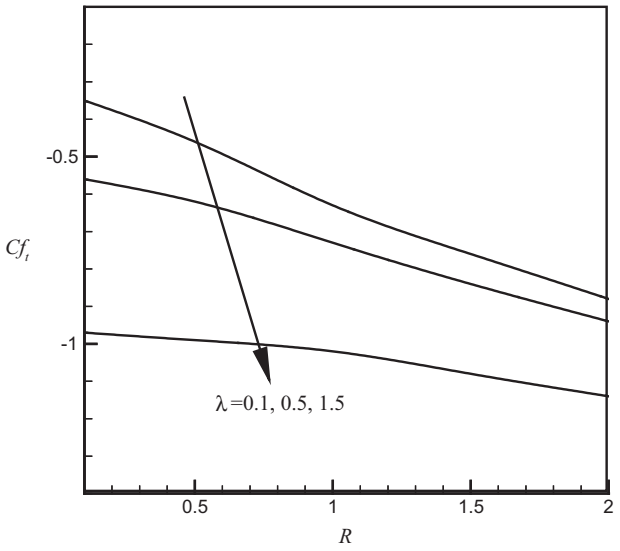

Figure 12 Cf_t versus R for different values of λ.

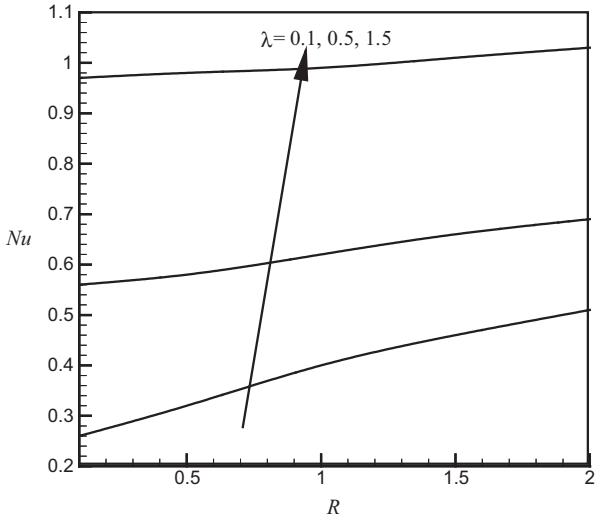

Figure 13 Nu versus R for different values of λ.

Table 3 Variation of Stanton number (or inward axial thermophoretic deposition velocity) for different values of Sc at $Pr = 0.71, \kappa = 0.5, N_t = 0.1, R = 1.0$ and $\lambda = 0.5$.

Sc	0.22	0.60	0.94	100	1000	2000
$St = -V_d^*$	2.6527073	1.0265275	0.6850266	0.0416088	0.0297816	0.0194139

thermophoretic force drives more particles closer to the disk so to decrease the concentration somewhere far from the cold surface.

Figs. 7 and 8 show typical concentration profiles across the boundary layer for various values of the Schmidt number Sc. From Fig. 7 it is clear that the concentration boundary layer thickness decreases as the Schmidt number Sc increases and this is analogous to the effect of increasing the Prandtl number on the thickness of a thermal boundary layer. Fig. 8, plotted for large values of Sc, shows that increase of these profiles is very steep for large Schmidt number. From the physical point of view, for smaller values of the Schmidt number, Brownian diffusion effect is more important as compared to the convection effect. However, for a large value of $Sc(> 1000)$ the diffusion effect is minimal as compared to the convection effect and therefore, the effect of thermophoresis alters the concentration boundary layer significantly.

In Fig. 9 we have shown the non-dimensional axial thermophoretic velocity $\left(W_T^*\right)$ versus κ for different values of thermophoresis parameter N_t. This figure reveals that axial thermophoretic velocity increases linearly with the increase of κ as well as with the increase of thermophoresis parameter N_t. Larger values of these parameters produce an increasing effect on W_T^* which is consistent with the work of Rahman and Postelnicu [22].

The combined effects of rotational parameter R as well as unsteadiness parameter λ on the non-dimensional axial thermophoretic velocity $\left(W_T^*\right)$ are displayed in Fig. 10. From this figure we observe that the thermophoretic velocity increases linearly with the increase of R as well as with the increase of unsteadiness parameter λ. This means that the rotational parameter R as well as unsteadiness parameter λ enhances the axial thermophoretic velocity.

The variation of the radial and tangential skin-frictions and the rate of heat transfer for some selected values of the unsteadiness parameter λ with rotational parameter R are displayed in Figs. 11–13 respectively. From these figures we see that both radial and tangential skin-frictions decrease whereas the rate of heat transfer increases with increasing values of the unsteadiness parameter λ.

Finally, Table 3 shows the variations of local Stanton number for different values of the Schmidt number Sc. This table confirms that the local Stanton number decreases as the Schmidt number increases. From this table it is also clear that the effect of larger Schmidt number leads asymptotically to a zero thermophoretic deposition velocity. This is in agreement with the physical explanations, based on the fact that the Schmidt number is the ratio of momentum diffusivity to Brownian diffusivity.

6. Conclusions

In this paper we have studied the effects of thermophoretic particle deposition on unsteady forced convective heat and mass transfer flow of a viscous incompressible fluid over a cold rapidly rotating disk. Using similarity transformations the governing nonlinear partial differential equations have been transferred into a system of ordinary differential equations that are solved numerically by applying Nachtsheim–Swigert shooting iteration technique along with sixth-order Runge–Kutta integration scheme. Comparison with previously published work for steady case of the problem was performed and found to be in very good agreement. From the present numerical investigations the following major conclusions may be drawn:

i. Radial, inward axial velocity and concentration profiles increase whereas both the tangential velocity and temperature profiles decrease with increasing values of the rotational parameter.
ii. Radial, tangential, inward axial velocity and temperature profiles decrease whereas concentration profiles increase with the increase of the unsteadiness parameter.
iii. Radial and tangential skin-frictions decrease whereas the rate of heat transfer increases with increasing values of the unsteadiness parameter.
iv. Concentration profiles decrease with the increase of thermophoretic coefficient and the thermophoresis parameter. On the other hand it increases with the increase of the Schmidt number.
v. Axial thermophoretic velocity increases linearly with the increase of thermophoretic coefficient, thermophoresis parameter, rotational parameter as well as unsteadiness parameter.
vi. Axial thermophoretic deposition flux decreases with the increase of the Schmidt number.

Acknowledgment

We would like to thank the anonymous referees for their valuable comments for further improvement of the paper. M. M. Rahman is grateful to the Sultan Qaboos University for funding through the research Grant IG/SCI/DOMS/13/05.

References

[1] von Karman T. Uber laminare und turbulente reibung. ZAMM 1921;1(4):233–5.
[2] Cochran WG. The flow due to a rotating disk. Proc Camb Philos Soc 1934;30(3):365–75.
[3] Benton ER. On the flow due to a rotating disk. Fluid Mech 1966;24(4):781–800.
[4] Millsaps K, Pohlhausen K. Heat transfer by laminar flow from a rotating disk. J Aerosp Sci 1952;19:120–6.
[5] Sparrow EM, Gregg JL. Mass transfer, flow, and heat transfer about a rotating disk. ASME J Heat Transf 1960:294–302.
[6] Attia HA. Unsteady MHD flow near a rotating porous disk with uniform suction or injection. Fluid Dyn Res 1998;23:283–90.

[7] Maleque KA, Sattar MA. Steady laminar convective flow with variable properties due to a porous rotating disk. ASME J Heat Transf 2005;127:1406–9.
[8] Attia HA. Steady flow over a rotating disk in porous medium with heat transfer. Nonlinear Anal Model Control 2009;14(1):21–6.
[9] Rahman MM. Convective hydromagnetic slip flow with variable properties due to a porous rotating disk. SQU J Sci 2010;15:55–79.
[10] Zueco J, Rubio V. Network method to study magnetohydrodynamic flow and heat transfer about rotating disk. Eng Appl Comput Fluid Mech 2012;6(3):336–45.
[11] Rahman MM. Thermophoretic deposition of nanoparticles due to a permeable rotating disk considering the effects of partial slip, magnetic field, thermal radiation, thermal-diffusion, and diffusion-thermo. World Acad Sci Eng Technol 2013;77, 2013-05-20.
[12] Goren SL. Thermophoresis of aerosol particles in laminar boundary layer on flat plate. J Colloid Interface Sci 1977;61:77–85.
[13] Talbot L, Cheng RK, Schefer AW, Willis DR. Thermophoresis of particles in a heated boundary layer. J Fluid Mech 1980;101:737–58.
[14] Mills AF, Hang X, Ayazi F. The effect of wall suction and thermophoresis on aerosol-particle deposition from a laminar boundary layer on a flat plate. Int J Heat Mass Transf 1984;27:1110–4.
[15] Jia G, Cipolla JW, Yener Y. Thermophoresis of a radiating aerosol in laminar boundary layer flow. J Thermophys Heat Transf 1992;6:476–82.
[16] Chiou MC, Cleaver JW. Effect of thermophoresis on submicron particle deposition from a laminar forced convection boundary layer flow on to an isothermal cylinder. J Aerosol Sci 1996;27:1155–67.
[17] Tsai R. A simple approach for evaluating the effect of wall suction and thermophoresis on aerosol particle deposition from a laminar flow over a flat plate. Int Commun Heat Mass Transf 1999;26:249–57.
[18] Postelnicu A. Effects of thermophoresis particle deposition in free convection boundary layer from a horizontal flat plate embedded in a porous medium. Int J Heat Mass Transf 2007;50:2981–5.
[19] Alam MS, Rahman MM, Sattar MA. Effects of variable suction and thermophoresis on steady MHD combined free-forced convective heat and mass transfer flow over a semi-infinite permeable inclined flat plate in the presence of thermal radiation. Int J Therm Sci 2008;47:758–65.
[20] Alam MS, Rahman MM, Sattar MA. Effects of chemical reaction and thermophoresis on MHD mixed convective heat and mass transfer flow along an inclined plate in the presence of heat generation/absorption with viscous dissipation and joule heating. Can J Phys 2008;86:1057–66.
[21] Alam MS, Rahman MM, Sattar MA. On the effectiveness of viscous dissipation and Joule heating on steady magnetohydrodynamic heat and mass transfer flow over an inclined radiate isothermal permeable surface in the presence of thermophoresis. Commun Nonlinear Sci Numer Simul. 2009;14:2132–43.
[22] Rahman MM, Postelnicu A. Effects of thermophoresis on the forced convective laminar flow of a viscous incompressible fluid over a rotating disk. Mech Res Commun 2010;37:598–603.
[23] Rahman ATM, Alam MS, Chowdhury MK. Thermophoresis particle deposition on unsteady two-dimensional forced convective heat and mass transfer flow along a wedge with variable viscosity and variable Prandtl number. Int Commun Heat Mass Transf 2012;39:541–50.
[24] Postelnicu A. Thermophoresis particle deposition in natural convection over inclined surfaces in porous media. Int J Heat Mass Transf 2012;55:2087–94.
[25] Batchelor GK, Shen C. Thermophoretic deposition of particles in gas flowing over cold surface. J Colloid Interface Sci 1985;107:21–37.
[26] Talbot L, Cheng RK, Schefer AW, Wills DR. Thermophoresis of particles in a heated boundary layer. J Fluid Mech 1980;101:737–58.
[27] Sattar MA, Hossain MM. Unsteady hydromagnetic free convection flow with hall current and mass transfer along an accelerated porous plate with time dependent temperature and concentration. Can J Phys 1992;70:369–74.
[28] Schlichting H. Boundary layer theory. McGraw Hill; 1968.
[29] Nachtsheim PR, Swigert P. Satisfaction of the asymptotic boundary conditions in numerical solution of the system of nonlinear equations of boundary layer type, NASA TND-3004; 1965.
[30] Alam MS, Rahman MM, Samad MA. Numerical study of the combined free-forced convection and mass transfer flow past a vertical porous plate in a porous medium with heat generation and thermal diffusion. Nonlinear Anal Model Control 2006;11:331–43.
[31] White FM. Viscous fluid flows. New York: McGraw-Hill, Inc.; 1991.
[32] Kelson N, Desseaux A. Note on porous rotating disk flow. ANZIAM J 2000;42(E):C837–55.

M.S. Alam was born in Naogaon, Bangladesh on 28th January 1971. He got his B.Sc. (Hons) in Mathematics and M.Sc. in Applied Mathematics from the Department of Mathematics, University of Dhaka. He also did M.Phil. in Mathematics from the Bangladesh University of Engineering and Technology (BUET), Dhaka in 2004. M.S. Alam obtained his Ph.D. degree in Applied Mathematics from the University of Dhaka in 2009 under the prudent supervision of Dr. Mohammad Mansur Rahman. His research interests include computational fluid dynamics, heat and mass transfer, non-Newtonian fluids and nano-fluidic phenomenon. Now, he is working as an Associate Professor in the Department of Mathematics, Jagannath University, Dhaka, Bangladesh. He supervised several graduate and undergraduate students. He has authored/co-authored around 50 research articles. M.S. Alam has hobbies to work with students, inventing new strategies of solving problems in fluid dynamics.

S.M. Chapal Hossain is working as an Assistant Professor in the Department of Mathematics, Jagannath University, Dhaka, Bangladesh. He obtained his M.Sc. degree in Applied Mathematics from the Department of Mathematics, University of Dhaka in 2006. Presently he is doing his M.Phil. in Mathematics from Bangladesh University of Engineering and Technology (BUET), Dhaka. He has around 10 research articles. His area of research interest is fluid dynamics.

M.M. Rahman was born in Pabna, Bangladesh, on 7th January 1973. He got his B.Sc. (Hons) in Mathematics and M.Sc. in Applied Mathematics from the Department of Mathematics, University of Dhaka, Bangladesh. For his outstanding results in B.Sc. (Hons) and M.Sc. examinations, he was awarded Raja Kalinarayan Scholarship (one of the most prestigious scholarships of the Dhaka University) and Asha Lata Sen Gold Medal, respectively. He got his Ph.D. in Applied Mathematics from the Department of

Mathematics, University of Glasgow, United Kingdom, in 2003 under the direction of Professor David R. Fearn, FRSE. His research interests include magnetohydrodynamics, mathematical fluid mechanics, nano-fluidic phenomena, heat and mass transfer, non-Newtonian fluids, transport in porous media, and bio-fluid flows.

Dr. Rahman is an Associate Professor in the Department of Mathematics and Statistics, Sultan Qaboos University, Sultanate of Oman. He has authored/co-authored around 80 research papers. Dr. Rahman has supervised one Ph.D., one M.Phil. (Co-supervision), 10 M.Sc. and several undergraduate students.

Dr. Rahman is a life member of Bangladesh Mathematical Society and Mathematics Students Alumni, University of Dhaka, Bangladesh.